Comparing Momentum and Support/Resistance Indicators: Rising Visibility Graphs, Linear Regression Channels, and DeMark TDST

William Bourgeois
william.bourgeois@mail.mcgill.ca
McGill University, School of Computer Science
Montreal, Quebec, Canada

Abstract

Many portfolio managers use heuristic indicators to decide when to buy or sell stocks. One popular indicator, Tom DeMark's Setup Trend (TDST), identifies price levels where stocks are expected to reverse direction (called support and resistance levels) and classifies the market as trending up or down (a momentum signal). Despite its widespread use, TDST has no formal statistical foundation. Its rules were developed through practitioner intuition rather than mathematical derivation.

This paper asks: **Do methods with stronger mathematical grounding produce better signals?** I compare three approaches on 93 large-cap equities over 10 years of daily data: TDST (the practitioner heuristic), Linear Regression Channels (a classical statistical method), and Rising Visibility Graphs (a graph-theoretic method from network science). Each method is evaluated on two tasks: momentum signal quality (measured by Information Coefficient and Forward Expectancy Tests) and support/resistance level accuracy (measured by error to realized price reversals and predictive power of level proximity).

The main findings are: (1) no method produces a reliable *momentum signal* at any tested horizon, a result that persists across all tested horizons and on both benchmark-normalized and raw prices, (2) LR and RVG *support/resistance levels* are roughly 40% more accurate than TDST, and (3) LR support levels show weak but statistically significant predictive power, though this effect is largely attributable to generic mean reversion rather than properties unique to the channel structure.

Keywords

rising visibility graphs, momentum indicators, support and resistance, information coefficient, DeMark TDST, technical analysis, financial time series, linear regression channels

1 Introduction

Portfolio managers need signals that tell them *which* stocks to overweight (relative to their benchmarks when applicable) and *where* prices are likely to reverse direction. A momentum signal ranks stocks by how strongly they are trending: a stock with positive momentum is expected to keep rising, while one with negative momentum is expected to keep falling. Support and resistance levels are specific prices where a stock is expected to stop falling (support) or stop rising (resistance). These concepts are central to technical analysis, the practice of using past price patterns to forecast future prices.

Tom DeMark's Setup Trend (TDST) is one of the most widely used technical indicators in institutional portfolio management [8]. It works by identifying patterns called "TD Setups": sequences of nine consecutive period closing prices that each move in the same direction relative to the price four periods earlier. When such a pattern completes, TDST marks the extreme price within that pattern as a support (min of setup where price increases) or resistance level (max of setup where price decreases.) The momentum signal is $+1$ when price crosses above resistance, -1 when below support, with the previous value held otherwise. This is one common interpretation rather than a definitive reading of DeMark's original intent, as practitioners vary in how they apply the indicator. Despite its popularity, TDST was developed through practitioner observation by Thomas DeMark [2], not derived from any statistical or mathematical framework.

This raises a natural question: *Do methods with stronger mathematical foundations produce better results?* I compare TDST against two alternatives. Linear Regression (LR) Channels fit ordinary least squares regression on log-prices within a rolling window, producing a trend line and statistical confidence bands that serve as support and resistance. Rising Visibility Graphs (RVGs), introduced by Zeng and Chen [9], are a graph-theoretic method from the network science literature. They construct a directed graph where nodes are price bars and edges connect bars that can "see" each other along rising price trajectories. I extract momentum and support/resistance signals from the topology of these graphs.

Each method produces two outputs: a momentum signal and a pair of support/resistance levels. I evaluate both outputs using four metrics from quantitative finance [3], applied uniformly across all three methods. The evaluation uses 93 large-cap equities over 10 years of daily data sourced from Bloomberg, with all prices normalized by the MSCI ACWI world index to isolate stock-specific behavior from broad market movements. This normalization is common practice among portfolio managers with a benchmark-relative mandate.

To my knowledge, no prior work applies Information Coefficient methodology to RVG-derived signals or benchmarks RVGs against TDST in a unified multi-asset framework.

2 Related Work

Lacasa et al. [4] introduced the Natural Visibility Graph (NVG), the direct ancestor of the RVG. In an NVG, bar i connects to bar j if the straight line between their (time, value) coordinates is not blocked by any intermediate bar. They showed that the degree distribution of the resulting graph encodes the autocorrelation structure of the underlying series.

Braga et al. [1] applied Horizontal Visibility Graphs to stock indices and showed that graph metrics correlate with financial instability. Liu and Chen [6] applied paired visibility and invisibility graphs to stock indices, demonstrating that node degree carries predictive information about return direction. Their finding motivates my choice of degree as a momentum proxy.

Zeng and Chen [9] introduced the Rising Visibility Graph (RVG), which restricts edges to positive-slope sight lines. This addresses a key limitation of standard NVGs: structural indistinguishability between rising and falling trends. I adopt RVG and its y-inverted counterpart as my graph construction, but depart from their kernel-based approach by using node degree as a scalar signal and evaluating under a unified IC framework.

Linear Regression Channels are a standard tool in quantitative finance. The Information Coefficient (IC), defined as the Spearman rank correlation between a signal and subsequent returns, is the standard evaluation metric for quantitative signals [3]. Lissandrin et al. [5] provide a rare empirical evaluation of DeMark indicators, finding statistically significant predictive power in only 6 of 21 commodity futures.

Gap addressed. No prior work has (1) derived continuous momentum signals and S/R levels from RVG topology, (2) evaluated them using IC methodology, or (3) compared them against TDST and LR Channels in a unified multi-asset framework.

3 Problem Definition

3.1 Formal Statement

Let $\tilde{P}_{t,i} = P_{t,i}/P_{t,\text{ACWI}}$ be the price of asset i relative to the MSCI ACWI benchmark, and $\mathcal{X}_{t,i} = \{\tilde{P}_{t-W+1,i}, \dots, \tilde{P}_{t,i}\}$ a rolling window of $W = 60$ bars. Each method $M \in \{\text{RVG}, \text{LR}, \text{TDST}\}$ maps $\mathcal{X}_{t,i}$ to a momentum signal $s^M_{t,i}$ and two price levels ($\text{sup}^M_{t,i}$, $\text{res}^M_{t,i}$). All outputs use only data available at time t. Returns are computed as $\tilde{r}_{t,i} = \tilde{P}_{t+N,i}/\tilde{P}_{t,i} - 1$, scaled by $\sigma_{t,i}$, a 60-bar rolling standard deviation estimated at $t-1$.

3.2 Signal Definitions

Table 1 summarizes all signal and level definitions. For TDST, the *true high* of a bar is $\max(\text{high}_t, \text{close}_{t-1})$ and the *true low* is $\min(\text{low}_t, \text{close}_{t-1})$.

Table 1: Signal and S/R level definitions for each method.

Method	Momentum $s_{t,i}$	Support	Resistance
RVG	$(k^+_t - k^-_t)/\sigma_{k^+-k^-}$ norm. degree diff.	Hub node in G^-	Hub node in G^+
LR	$\hat{\beta}/\sigma_{\hat{\beta}}$ OLS slope t-stat	$\exp(\hat{y}_t - 2\sigma_\varepsilon)$	$\exp(\hat{y}_t + 2\sigma_\varepsilon)$
TDST	$+1$ if $P > \text{res}$, -1 if $P < \text{sup}$	Lowest true low from sell setup	Highest true high from buy setup

3.3 Evaluation Metrics

Momentum quality is assessed by two metrics. The **Information Coefficient (IC)** is the Spearman rank correlation between each asset's signal and its subsequent N-bar volatility-scaled return, computed cross-sectionally at each date and averaged over non-overlapping periods. The IC answers: do higher signals predict higher returns? The **Forward Expectancy Test (FET)** pools all observations, splits them into positive-signal and negative-signal groups, and uses a Mann-Whitney U test to compare their return distributions. It answers: are returns different when the signal is positive vs. negative?

S/R level accuracy is assessed by two metrics. **MAE to reversal** finds the next price reversal of at least $\delta = 1.0\sigma$ within 20 bars and reports $|L - \text{reversal}|/\sigma$. Lower MAE means the predicted level is closer to where price actually turned. The **IC on level distance** computes $d = (L - P)/\sigma$ and tests its Spearman correlation with forward returns. A significant IC means proximity to a level has cross-sectional predictive power.

Figure 1 illustrates the mechanics of all four metrics on a single example date (only for visual aid, not representative of actual results).

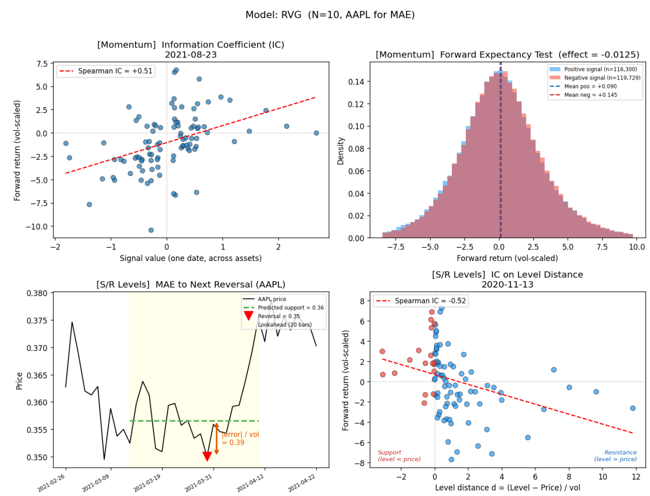

Figure 1: Visual overview of the four evaluation metrics.

4 Dataset

All data are retrieved from the Bloomberg Terminal via `blpapi`. The initial universe consists of 100 equities selected to approximate MSCI ACWI country and sector weights [7], covering February 2016 to February 2026 (≈2,610 trading days per asset). After applying a coverage filter (<20% missing data) and a staleness filter (<5% identical consecutive closes), 93 assets remain. Remaining gaps are forward-filled (up to 5 days), and all OHLC prices are divided by the MSCI ACWI close to produce benchmark-relative series.

Survivorship bias. The universe is selected from current (February 2026) ACWI constituents, so delisted companies are excluded. This affects absolute return levels but not relative method comparisons, because all three methods face the same bias and the evaluation uses rank-based metrics. In other words, survivorship bias is unlikely to materially affect the conclusions of this study because I am comparing methods against each other, not back-testing a trading strategy. The full asset list appears in the appendix.

5 Methodology

5.1 DeMark TDST (Practitioner Benchmark)

A TDST *setup* is nine consecutive closes each lower (buy setup) or higher (sell setup) than the close four bars earlier [2, 8]. Support is the lowest "true low" from the most recent sell setup. Resistance is the highest "true high" from the most recent buy setup. These levels update only when a new nine-bar setup completes, creating long periods of staleness. The momentum signal is +1 when price crosses above resistance, −1 when below support, with the previous value held otherwise. This is one common institutional interpretation rather than a definitive reading of DeMark's original intent, as practitioners vary in how they apply the indicator. TDST has no adjustable window parameter.

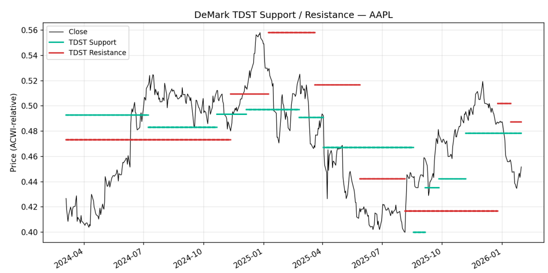

Figure 2: TDST support and resistance levels for AAPL (ACWI-relative). Levels update only when a new nine-bar setup completes, creating a characteristic staircase pattern.

5.2 Linear Regression Channels (Statistical Baseline)

A rolling OLS regression is fit on $\log \tilde{P}_{t,i}$ within a trailing window of W bars: $\log \tilde{P}_{t,i} = \alpha + \hat{\beta} \cdot t + \varepsilon_t$. The momentum signal is $s_{t,i} = \hat{\beta}/\sigma_{\hat{\beta}}$, the slope t-statistic. Support and resistance are $\exp(\hat{y}_t \mp 2\sigma_\varepsilon)$. Under homoskedastic residuals, approximately 95% of prices lie within the channel. The channel updates every bar as the window slides forward.

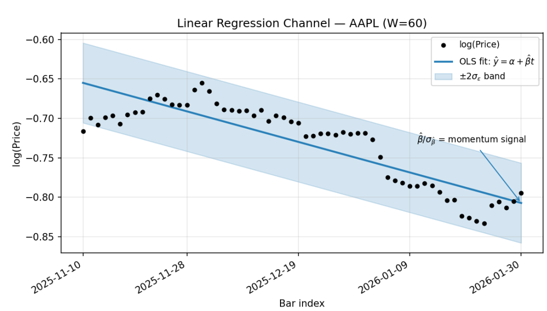

Figure 3: Single-window OLS fit on log(price) for AAPL (W = 60). The blue band is the $\pm 2\sigma_\varepsilon$ channel. The slope's t-statistic is the momentum signal for this window.

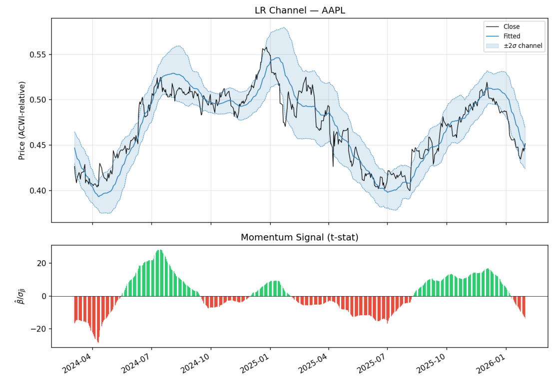

Figure 4: Rolling LR channel (top) and momentum signal (bottom) for AAPL. The channel updates every bar, tracking the current trend tightly.

5.3 Rising Visibility Graphs (Graph-Theoretic Method)

At each date t, two graphs are constructed over $\mathcal{X}_{t,i}$ using the RVG algorithm [9]. In G^+ (the Rising VG), nodes represent price bars and an edge connects bar i to bar j ($i < j$) only if the straight line between them has positive slope *and* is not blocked by any intermediate bar. In G^- (the Inverted RVG), the same algorithm is applied to $-\tilde{P}_{t,i}$, so that troughs become peaks and downward structure is captured.

From each graph, the **last-node degree** (k_t^+ from G^+, k_t^- from G^-) measures how many preceding bars the current bar can see through rising (or falling) sight lines. The momentum signal is $(k_t^+ - k_t^-)/\sigma_W(k^+ - k^-)$. If price has been rising, the current bar sits high with many upward sight lines (k^+ large, k^- small), yielding a positive signal. Support is the price at the highest-degree hub node in G^- (the dominant trough). Resistance is the price at the hub of G^+ (the dominant peak). Figure 5 illustrates the paired construction, and Figure 6 shows the rolling signals over time.

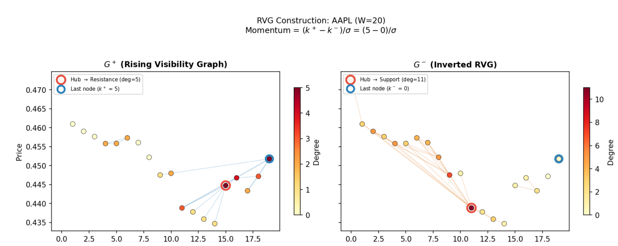

Figure 5: Paired RVG construction for AAPL (W = 20). Left: G^+ with rising visibility edges. The hub node (red circle, highest degree) defines resistance. Right: G^- on inverted prices, its hub defines support. Node colour encodes degree.

6 Experiment Setup

Window size $W = 60$ (approximately one calendar quarter). Robustness checks use $W \in \{20, 60, 120\}$. **Forward horizons** $N \in$

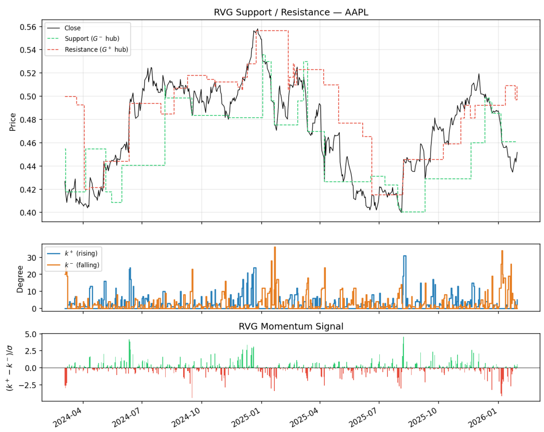

Figure 6: RVG rolling view for AAPL: price with hub-based S/R levels (top), last-node degrees k^+ and k^- (middle), and normalized momentum signal (bottom).

$\{5, 10, 20\}$ bars with non-overlapping subsampling to prevent autocorrelation. **TDST** uses DeMark's original fixed rules with no adjustable parameters.

Addressing non-stationarity. Cross-sectional IC is computed by ranking assets against each other on the same date, so market-wide trends cancel out. Forward returns are divided by rolling volatility to remove heteroskedasticity. Together, these ensure comparability across time periods [3].

7 Results

7.1 Momentum Signal Quality

7.1.1 Information Coefficient. Table 2 reports the IC for each method and horizon. Across all methods and horizons, the IC is indistinguishable from zero. The largest absolute mean IC is 0.010 (RVG at $N = 10$), and no t-statistic exceeds 2.0 in magnitude. Figure 7 visualizes these results.

Table 2: Information Coefficient on momentum signals. No method achieves $|t| > 2$.

Method	N	IC	Std	t
TDST	5	−0.005	0.196	−0.55
TDST	10	−0.003	0.192	−0.26
TDST	20	+0.000	0.179	+0.01
LR	5	−0.003	0.217	−0.31
LR	10	+0.000	0.222	+0.02
LR	20	+0.007	0.212	+0.35
RVG	5	−0.005	0.197	−0.53
RVG	10	−0.010	0.217	−0.70
RVG	20	+0.005	0.188	+0.32

7.1.2 Forward Expectancy Test. Table 3 reports FET results. TDST and LR show no significant separation between positive and negative signal regimes (all $p > 0.18$). RVG produces two significant results at $N = 5$ and $N = 10$, but the sign is *negative*: assets with positive RVG signals tend to underperform.

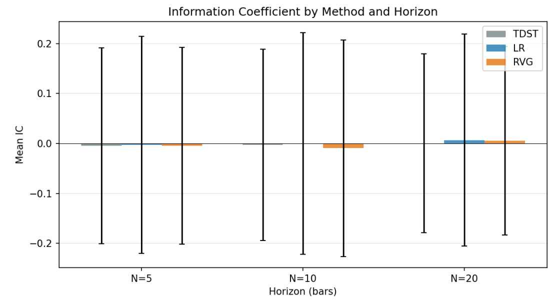

Figure 7: Mean IC by method and horizon. All values are near zero with wide error bands, indicating no reliable predictive power for any momentum signal.

Table 3: Forward Expectancy Test. $p < 0.05$ marked with *.

Method	N	$\bar{r}^+$	$\bar{r}^-$	Effect	p
TDST	5	.060	.056	−.003	.63
TDST	10	.124	.106	+.000	.99
TDST	20	.266	.200	+.008	.49
LR	5	.062	.057	−.001	.88
LR	10	.137	.095	+.004	.58
LR	20	.286	.176	+.014	.18
RVG	5	.045	.073	$-.014^*$	.008
RVG	10	.080	.152	$-.020^*$	.008
RVG	20	.264	.203	+.003	.77

7.1.3 The RVG Signal Is a Past-Return Proxy. The RVG FET result appears noteworthy, so I investigated whether the signal is genuinely novel or a complex encoding of something simpler. In a Natural Visibility Graph, the last node's edges are dominated by *recent* bars because distant bars are almost always blocked by intermediate ones. Empirically, the median edge distance from the last node is only 8 bars (measured across 128 sampled dates for AAPL), and 56% of edges fall within 10 bars. This means $k^+ - k^-$ effectively measures recent price direction over roughly 10 bars, not the full 60-bar window.

Five tests confirm this interpretation. (A) The cross-sectional Spearman correlation between the RVG signal and the simple 10-bar past return is $\rho = 0.39$, versus only 0.16 with the 60-bar past return. (B) A trivial 10-bar past return signal produces an FET effect of −0.020 ($p = 0.007$), nearly identical to the RVG result. (C) The FET effect is significant in the first half (2016 to 2021, $p = 0.003$) but vanishes in the second half (2021 to 2026, $p = 0.32$). (D) Only 4 of 10 subsampling offsets produce $p < 0.05$. (E) The cross-sectional Spearman correlation between RVG signals computed at $W = 20$, 60, and 120 exceeds 0.95, confirming that the signal barely changes with window size.

In summary, the RVG momentum signal is a nonlinear encoding of recent price direction. Its negative FET effect is short-term mean reversion, not a novel graph-theoretic discovery. This also explains why the RVG FET rows appear nearly identical across window sizes in the robustness analysis: the signal is governed by the last $\sim$10 bars regardless of W.

7.1.4 Explaining the Null Momentum Result. The null IC across all three methods raises the question: is this a flaw in the signal designs, or something about the data?

To rule out signal design, I tested two additional practitioner baselines. A moving average crossover computes two rolling averages of the price, one short-term and one long-term, and signals +1 when the short average is above the long average (uptrend) and −1 otherwise. I tested both a simple moving average (SMA) and an exponential moving average (EMA, which gives more weight to recent prices), each using a 10-bar short window and a 60-bar long window (denoted 10/60). Neither achieves a significant IC or FET effect at any tested horizon (all $|t| < 0.74$, all $p > 0.19$). The null is not specific to any one method. Full results appear in Appendix C.

To rule out horizon choice, I tested all five signals at extended horizons of $N = 60$, 120, and 250 bars (approximately 3, 6, and 12 months). No signal achieves $|t| > 2.0$ even at these longer horizons. To rule out benchmark normalization as the cause, I repeated the IC tests on raw (unnormalized) prices. The null persists.

The result is therefore robust across signal designs, horizons, and price transformations. These momentum signals do not carry cross-sectional predictive power for this equity universe over the study period. The cause remains an open question: possibilities include the large-cap composition of the universe (momentum effects are often stronger in smaller stocks) and the long sample period (10 years may average over alternating momentum and reversal regimes).

7.2 Support/Resistance Level Accuracy

7.2.1 MAE to Next Realized Reversal. Table 4 reports the MAE results at $\delta = 1.0\sigma$. LR and RVG levels are substantially more accurate than TDST, with roughly 40% lower normalized MAE. The standard deviations are also roughly 30% lower, meaning LR and RVG are not only more accurate on average but also more consistent. The difference is structural: TDST levels update only upon completion of a nine-bar setup and can remain stale for extended periods, while LR and RVG update every bar. Between LR and RVG, accuracy is similar. Figure 8 illustrates the three methods' S/R levels.

Table 4: MAE to reversal ($\delta = 1.0\sigma$, 20-bar lookahead). Lower is better.

Method	Level	MAE	Std
TDST	Support	4.25	7.21
TDST	Resistance	4.49	8.16
LR	Support	2.70	4.92
LR	Resistance	2.90	5.47
RVG	Support	2.67	5.55
RVG	Resistance	2.52	5.23

Qualifying-reversal rates. The MAE metric excludes observations where no qualifying reversal occurs within 20 bars. If TDST were excluded at a higher rate than LR/RVG, a sample selection bias could shrink the apparent gap. I verified that qualifying rates are nearly identical across methods: all three find reversals in approximately 63.2% of level observations at $\delta = 1.0\sigma$, so differential exclusion does not bias the comparison.

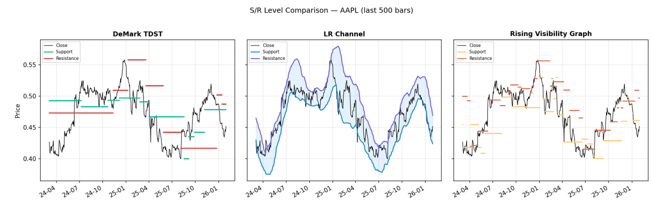

Figure 8: Side-by-side S/R levels for AAPL. TDST levels (left) show long flat segments between setup completions. LR (center) and RVG (right) track price more closely.

7.2.2 IC on Level Distance. Table 5 reports the IC on level distance. The most striking finding is an asymmetry between support and resistance. LR support produces significant ICs at all three horizons ($t = 2.25$, 2.05, 2.10), the only method-level combination to achieve consistent significance. RVG resistance is borderline significant at $N = 5$ ($t = 2.12$) but does not persist at longer horizons. No TDST level achieves significance.

Table 5: IC on level distance. $|t| > 2$ in bold.

Meth.	Level	N	IC	Std	t
TDST	Sup	5	.008	.197	0.90
TDST	Sup	10	.010	.196	0.81
TDST	Sup	20	.013	.193	0.76
TDST	Res	5	.005	.193	0.62
TDST	Res	10	.004	.188	0.33
TDST	Res	20	.006	.186	0.37
LR	Sup	5	.018	.178	**2.25**
LR	Sup	10	.024	.186	**2.05**
LR	Sup	20	.032	.172	**2.10**
LR	Res	5	.008	.175	0.97
LR	Res	10	.010	.179	0.86
LR	Res	20	.010	.178	0.61
RVG	Sup	5	.009	.190	1.10
RVG	Sup	10	.011	.186	0.91
RVG	Sup	20	.019	.181	1.19
RVG	Res	5	.018	.187	**2.12**
RVG	Res	10	.021	.181	1.80
RVG	Res	20	.020	.185	1.23

For support, d is typically negative because the level sits below the current price. The positive IC means that a less negative d (price closer to support) is associated with higher forward returns. In other words, assets trading near their lower channel boundary tend to bounce rather than break through, consistent with a mean-reversion effect at support.

7.2.3 LR Support IC vs. Mean-Reversion Baseline. An asset trading near its lower LR channel boundary has by construction recently underperformed its own trend. The LR support IC could therefore reflect generic short-term mean reversion rather than anything specific to the channel as a support level. To test this, I constructed a "naive mean-reversion signal" as $d_{\text{MR}} = -(\text{past } N\text{-bar return})/\sigma$ and computed its IC on forward returns using the same methodology. Table 6 reports the results.

Table 6: LR support distance IC vs. mean-reversion baseline. Wilcoxon $p > 0.05$ at all horizons.

N	LR IC	MR IC	ΔIC	p
5	0.018	0.008	+0.010	0.529
10	0.024	0.020	+0.004	0.793
20	0.032	0.013	+0.019	0.231

Table 6 shows that the difference between the LR support IC and the mean-reversion IC is not statistically significant at any horizon (paired Wilcoxon $p > 0.23$). The LR support IC is largely a mean-reversion effect: assets near recent lows tend to bounce. This does not invalidate the practical result, since the signal works regardless of the underlying mechanism. The LR channel remains a useful tool for identifying those lows in a principled and interpretable way.

7.2.4 Support/Resistance Asymmetry. The finding that support IC is significant while resistance IC is not is an interesting result in this study. I investigate its robustness through three conditioning analyses, all at $N = 10$.

(A) Recent return sign. Among assets that recently rose (positive 20-bar return), the LR support IC remains significant ($t = 2.17$). Among recent decliners it weakens ($t = 1.14$). Resistance IC is insignificant in both groups ($t = 0.61$ and $t = 0.46$). The asymmetry holds in both subsamples, and the support effect is not simply a mechanical consequence of recent losses.

(B) Market regime. In bull markets (positive 60-bar rolling mean return), LR support IC is strong ($t = 2.66$) while resistance remains insignificant ($t = 1.06$). In bear markets ($n = 40$ dates), both support and resistance lose significance ($t = -0.95$ and $t = -0.35$). The support effect appears concentrated in bull regimes, consistent with the idea that institutional "buy the dip" behavior at the lower channel boundary is more systematic during up-trending markets.

(C) Volatility. The support IC is strongest among high-volatility assets ($t = 2.18$) and weakest among low-volatility assets ($t = 0.54$). Resistance shows no consistent pattern across volatility groups ($t = -0.95, 1.78, 0.54$ for high, mid, and low volatility). One tentative explanation is that high-volatility assets are more likely to touch the lower channel boundary and therefore generate more "dip" opportunities, while no analogous mechanism exists at the upper boundary. However, the bear-market fragility (finding B) cautions against over-interpreting this as a stable structural phenomenon.

7.2.5 Richer RVG Graph Features. The main analysis reduces the full RVG to a single scalar (last-node degree difference). To bound claims appropriately, I tested whether richer graph-derived features carry incremental momentum information. I computed four additional features from G^+ and G^-: mean degree difference, degree entropy difference, hub age difference (how many bars ago the dominant peak/trough occurred), and hub degree ratio difference. None of these achieves $|t| > 2$ at any horizon. The null momentum result extends to multiple RVG-derived features, not just the specific last-node degree signal. I note, however, that this does not rule out usefulness of more sophisticated graph features (e.g., Weisfeiler-Lehman kernels as in [9]) that are outside the scope of this study.

7.3 Robustness

I re-ran LR and RVG signal generation at $W = 20$ and $W = 120$ and re-evaluated all four metrics. Key findings: (1) momentum ICs remain near zero for all methods and windows, (2) the LR/RVG accuracy advantage over TDST persists across all window sizes, (3) the LR support IC on level distance remains at or near significance ($t = 1.69, 2.14, 1.94$ for $W = 20, 60, 120$). Full robustness tables are provided in the appendix.

8 Discussion

Momentum signals do not work in this universe. The null IC across all three methods and two additional moving-average baselines confirms that none of these signals carry cross-sectional predictive power. The null persists across short and long horizons and on both benchmark-normalized and raw prices. The cause remains open, but the large-cap composition of the universe and the 10-year averaging window are plausible contributing factors. Regardless of the cause, the practical implication is clear: none of the tested signals should be used as standalone momentum indicators for this type of equity portfolio.

S/R levels are the useful output. The primary practical value from all three methods is the support and resistance level itself, not the directional momentum score. LR and RVG produce levels roughly 40% closer to actual price turning points than TDST, with roughly 30% lower variance in prediction error. This advantage is robust across window sizes and reversal thresholds. The LR support IC on level distance (≈ 0.02 to 0.03) suggests a weak but real mean-reversion effect at the lower channel boundary. However, this effect is largely indistinguishable from a simple past-return signal (Section 7.2.3), and is concentrated in bull markets (Section 7.2.4).

The support/resistance asymmetry. This is an interesting finding. Support produces significant predictive IC while resistance does not. The conditioning analyses in Section 7.2.4 show that this gap persists across return subgroups and volatility quintiles, with resistance IC remaining insignificant in every partition tested. One explanation is that buying near support ("buy the dip") is a more systematic institutional behavior than selling near resistance, where profit-taking decisions depend on portfolio-specific factors like tax lots and rebalancing schedules. The bull-market concentration of the support effect reinforces this: dip-buying is most consistent when the broader trend is upward. However, the bear-market fragility prevents me from making a strong claim about structural permanence. A deeper investigation of this asymmetry with longer samples and different asset classes is left for future work.

Transaction costs. The LR support IC of 0.024 is statistically significant but small in magnitude. A rough estimate using the

Grinold-Kahn framework [3] suggests that a portfolio trading solely on this signal would need transaction costs below approximately 3 basis points per trade to remain profitable, well below the 5 to 15 basis points typical of institutional large-cap trading. In practice, this means the LR support signal is unlikely to generate profits on its own. It is better understood as one input among many in a broader investment process, complementing fundamental research and other quantitative signals rather than serving as the sole basis for trading decisions.

What the RVG contributes. RVG achieves comparable MAE to LR on S/R levels, which shows that a graph-theoretic method with no statistical assumptions can approach the precision of classical OLS. However, LR support is the only level with consistently significant predictive IC, giving LR the overall advantage. The RVG momentum signal reduces to a proxy for recent price direction (Section 7.1.3). More sophisticated uses of the graph structure (e.g., kernel methods [9]) remain a promising direction.

9 Conclusions

I compared three approaches to momentum and support/resistance estimation on 93 equities over 10 years: DeMark TDST (practitioner heuristic), Linear Regression Channels (statistical baseline), and Rising Visibility Graphs (graph-theoretic method from network science).

No method produces a reliable momentum signal at any tested horizon, including extended horizons up to 12 months. The null persists on both benchmark-normalized and raw prices, and across all five signal designs tested. The cause remains an open question.

For support and resistance levels, LR and RVG substantially outperform TDST, with roughly 40% lower error to realized reversals and 30% lower standard deviation in those errors. LR support levels show a weak but significant predictive relationship with forward returns, though this is largely attributable to mean reversion and is stronger in bull markets.

The most novel finding is the support/resistance asymmetry: support levels carry weak predictive power while resistance levels do not. This pattern is consistent across methods and conditioning analyses.

For the network science community: the RVG achieves competitive S/R accuracy through pure graph topology, but its momentum signal in the tested form reduces to a short-horizon past-return proxy. Richer graph features (Section 7.2.5) did not resolve this limitation, though more advanced graph-theoretic approaches remain unexplored.

For practitioners: LR channel boundaries outperform TDST levels on every metric tested, producing 40% lower error, 30% lower standard deviation, and the only statistically significant predictive IC in the study, all while updating continuously and offering a transparent statistical interpretation.

References

[1] Antônio Carlos Braga et al. 2017. Statistical validation of financial time series via visibility graph. arXiv:1710.10980

[2] Thomas R. DeMark. 1994. *The New Science of Technical Analysis*. Wiley.

[3] Richard C. Grinold and Ronald N. Kahn. 1999. *Active Portfolio Management* (2nd ed.). McGraw-Hill.

[4] Lucas Lacasa, Bartolo Luque, Fernando Ballesteros, Jordi Luque, and Juan Carlos Nuno. 2008. From time series to complex networks: The visibility graph. *Proceedings of the National Academy of Sciences* 105, 13 (2008), 4972–4975. doi:10.1073/pnas.0709247105

[5] Marco Lissandrin, Fionn Daly, and Didier Sornette. 2017. *Statistical Testing of DeMark Indicators in Commodity Futures Markets*. Master's thesis. ETH Zurich.

[6] Ruiyun Liu and Yu Chen. 2020. Analysis of Stock Price Motion Asymmetry via Visibility-Graph Algorithm. *Frontiers in Physics* 8 (2020). doi:10.3389/fphy.2020.539521

[7] MSCI Inc. 2026. MSCI ACWI Index Factsheet. Available at https://www.msci.com/indexes/index/892400.

[8] Jason Perl. 2008. *DeMark Indicators*. Bloomberg Press. Foreword by Thomas R. DeMark.

[9] Zhixiang Zeng and Yu Chen. 2025. Forecasting Stock Price Patterns with a Rising Visibility Graph Based Method. *Forecasting* 7, 2 (2025), 26. doi:10.3390/forecast7020026

A Investment Universe

The 100-asset universe was constructed to approximate the MSCI ACWI index in terms of both country and sector representation, using the February 2026 ACWI factsheet as a reference [7]. Country weights were treated as the primary constraint: the USA (61.63%) receives 62 stocks, Japan (5.39%) receives 5, the UK (3.45%) receives 3, Canada (3.13%) receives 3, China (2.87%) receives 3, and the remaining 23.52% receives 24 stocks distributed across France, Germany, Switzerland, Australia, Taiwan, India, South Korea, Netherlands, Denmark, Sweden, Norway, Spain, Singapore, Israel, Italy, and Brazil. Within each country block, stocks were selected to approximate ACWI sector weights as closely as practical, prioritizing the largest constituents by market capitalization.

After data quality filtering (Section 4), 7 assets were removed and 93 remain. Table 7 lists the final universe.

B Robustness: Full Results Across Windows and Horizons

This appendix reports the complete results of the window sensitivity analysis. All metrics are recomputed for LR and RVG at $W \in \{20, 60, 120\}$, with TDST included once (it is window-invariant). Table 8 reports momentum IC, Table 9 reports FET results, Table 10 reports MAE to reversal, and Table 11 reports IC on level distance.

C SMA/EMA Baseline Results

Simple and exponential moving average crossovers are among the most widely used practitioner signals. Although they were not included in the main comparison (moving averages produce no support and resistance levels), both are tested here on the momentum-only metrics to confirm that the null IC result is not specific to the three main methods.

Table 12 shows that neither SMA nor EMA crossover achieves a significant IC or FET effect at any horizon. This confirms that the null momentum result is not specific to the three main methods (see Section 7.1.4).

Table 7: Final 93-asset investment universe after quality filtering. Seven assets from the original 100 were excluded: AZN, NU, PDD, TTE, XP (coverage) and SAN, UMC (staleness).

Ticker	Country	Sector
NVDA US EQUITY	USA	Info Tech
AAPL US EQUITY	USA	Info Tech
MSFT US EQUITY	USA	Info Tech
AVGO US EQUITY	USA	Info Tech
AMD US EQUITY	USA	Info Tech
ORCL US EQUITY	USA	Info Tech
CRM US EQUITY	USA	Info Tech
ADBE US EQUITY	USA	Info Tech
CSCO US EQUITY	USA	Info Tech
TXN US EQUITY	USA	Info Tech
QCOM US EQUITY	USA	Info Tech
ACN US EQUITY	USA	Info Tech
INTC US EQUITY	USA	Info Tech
AMAT US EQUITY	USA	Info Tech
KLAC US EQUITY	USA	Info Tech
LRCX US EQUITY	USA	Info Tech
JPM US EQUITY	USA	Financials
BAC US EQUITY	USA	Financials
BRK/B US EQUITY	USA	Financials
V US EQUITY	USA	Financials
MA US EQUITY	USA	Financials
GS US EQUITY	USA	Financials
MS US EQUITY	USA	Financials
WFC US EQUITY	USA	Financials
AXP US EQUITY	USA	Financials
BLK US EQUITY	USA	Financials
CAT US EQUITY	USA	Industrials
HON US EQUITY	USA	Industrials
RTX US EQUITY	USA	Industrials
GE US EQUITY	USA	Industrials
UNP US EQUITY	USA	Industrials
DE US EQUITY	USA	Industrials
LMT US EQUITY	USA	Industrials
AMZN US EQUITY	USA	Cons. Discr.
TSLA US EQUITY	USA	Cons. Discr.
HD US EQUITY	USA	Cons. Discr.
MCD US EQUITY	USA	Cons. Discr.
NKE US EQUITY	USA	Cons. Discr.
BKNG US EQUITY	USA	Cons. Discr.
JNJ US EQUITY	USA	Health Care
LLY US EQUITY	USA	Health Care
UNH US EQUITY	USA	Health Care
ABBV US EQUITY	USA	Health Care
MRK US EQUITY	USA	Health Care
TMO US EQUITY	USA	Health Care
GOOGL US EQUITY	USA	Comm. Services

Ticker	Country	Sector
META US EQUITY	USA	Comm. Services
NFLX US EQUITY	USA	Comm. Services
DIS US EQUITY	USA	Comm. Services
VZ US EQUITY	USA	Comm. Services
WMT US EQUITY	USA	Cons. Staples
PG US EQUITY	USA	Cons. Staples
KO US EQUITY	USA	Cons. Staples
COST US EQUITY	USA	Cons. Staples
XOM US EQUITY	USA	Energy
CVX US EQUITY	USA	Energy
COP US EQUITY	USA	Energy
LIN US EQUITY	USA	Materials
NEM US EQUITY	USA	Materials
NEE US EQUITY	USA	Utilities
DUK US EQUITY	USA	Utilities
PLD US EQUITY	USA	Real Estate
TM US EQUITY	Japan	Cons. Discr.
SONY US EQUITY	Japan	Comm. Services
MUFG US EQUITY	Japan	Financials
TOELY US EQUITY	Japan	Info Tech
FANUY US EQUITY	Japan	Industrials
SHEL US EQUITY	UK	Energy
HSBC US EQUITY	UK	Financials
SHOP US EQUITY	Canada	Info Tech
RY US EQUITY	Canada	Financials
CNQ US EQUITY	Canada	Energy
TCEHY US EQUITY	China	Comm. Services
BABA US EQUITY	China	Cons. Discr.
LVMUY US EQUITY	France	Cons. Discr.
BNPQY US EQUITY	France	Financials
SAP US EQUITY	Germany	Info Tech
SIEGY US EQUITY	Germany	Industrials
RHHBY US EQUITY	Switzerland	Health Care
NSRGY US EQUITY	Switzerland	Cons. Staples
BHP US EQUITY	Australia	Materials
ANZGY US EQUITY	Australia	Financials
TSM US EQUITY	Taiwan	Info Tech
HDB US EQUITY	India	Financials
INFY US EQUITY	India	Info Tech
SKHSY US EQUITY	S. Korea	Info Tech
ASML US EQUITY	Netherlands	Info Tech
NVO US EQUITY	Denmark	Health Care
ERIC US EQUITY	Sweden	Info Tech
EQNR US EQUITY	Norway	Energy
DBSDY US EQUITY	Singapore	Financials
CHKP US EQUITY	Israel	Info Tech
ENLAY US EQUITY	Italy	Utilities

Table 12: Moving average crossover baselines (not part of main comparison). All $|t| < 1$ and $p > 0.19$.

Signal	N	IC	t	FET eff.	p
SMA 10/60	5	−.006	−.74	−.007	.19
SMA 10/60	10	−.006	−.51	−.007	.38
SMA 10/60	20	−.010	−.62	−.007	.53
EMA 10/60	5	.000	.00	+.001	.93
EMA 10/60	10	−.001	−.05	+.001	.88
EMA 10/60	20	.001	.06	+.005	.67

Table 8: Full momentum IC results across all windows and horizons.

W	Method	N	Mean IC	Std IC	t-stat	Count
20	LR	5	−0.012	0.205	−1.28	496
20	LR	10	−0.013	0.204	−1.00	247
20	LR	20	−0.017	0.199	−0.97	123
20	RVG	5	−0.004	0.195	−0.48	496
20	RVG	10	−0.012	0.215	−0.90	247
20	RVG	20	+0.009	0.190	+0.54	123
60	LR	5	−0.002	0.219	−0.23	496
60	LR	10	+0.001	0.224	+0.05	247
60	LR	20	+0.009	0.214	+0.44	123
60	RVG	5	−0.004	0.196	−0.50	496
60	RVG	10	−0.012	0.217	−0.87	247
60	RVG	20	+0.002	0.187	+0.12	123
120	LR	5	+0.004	0.242	+0.39	496
120	LR	10	+0.001	0.242	+0.08	247
120	LR	20	+0.006	0.227	+0.29	123
120	RVG	5	−0.006	0.196	−0.69	496
120	RVG	10	−0.015	0.216	−1.08	247
120	RVG	20	−0.003	0.188	−0.18	123
N/A	TDST	5	−0.003	0.197	−0.28	496
N/A	TDST	10	−0.001	0.193	−0.09	247
N/A	TDST	20	+0.003	0.181	+0.18	123

Table 9: Full FET results across all windows and horizons. $p < 0.05$ marked with *. RVG rows are numerically near-identical across windows because the signal is governed by the last ~10 bars regardless of W (see Section 7.1.3).

W	Method	N	Mean$^+$	Mean$^-$	Effect	p-value
20	LR	5	0.042	0.071	−0.010	0.077
20	LR	10	0.081	0.148	−0.013	0.081
20	LR	20	0.141	0.321	−0.023*	0.035
20	RVG	5	0.041	0.070	−0.014*	0.008
20	RVG	10	0.067	0.161	−0.020*	0.005
20	RVG	20	0.241	0.219	+0.001	0.949
60	LR	5	0.060	0.052	+0.001	0.871
60	LR	10	0.131	0.097	+0.004	0.562
60	LR	20	0.277	0.180	+0.014	0.192
60	RVG	5	0.041	0.070	−0.014*	0.008
60	RVG	10	0.067	0.161	−0.020*	0.005
60	RVG	20	0.241	0.219	+0.001	0.949
120	LR	5	0.054	0.058	+0.001	0.863
120	LR	10	0.116	0.112	−0.002	0.777
120	LR	20	0.240	0.219	+0.001	0.907
120	RVG	5	0.041	0.070	−0.013*	0.020
120	RVG	10	0.067	0.161	−0.018*	0.017
120	RVG	20	0.241	0.219	+0.005	0.657
N/A	TDST	5	0.055	0.057	−0.002	0.731
N/A	TDST	10	0.118	0.113	−0.001	0.938
N/A	TDST	20	0.253	0.214	+0.006	0.555

Table 10: Full MAE to reversal across all windows ($\delta = 1.0\sigma$).

W	Method	Level	Mean MAE	Std MAE	Count
20	LR	Support	1.70	3.24	145 034
20	LR	Resistance	1.76	3.42	145 034
20	RVG	Support	1.57	3.16	145 034
20	RVG	Resistance	1.55	3.38	145 034
60	LR	Support	2.70	4.97	145 034
60	LR	Resistance	2.91	5.43	145 034
60	RVG	Support	2.66	5.35	145 034
60	RVG	Resistance	2.52	5.26	145 034
120	LR	Support	3.65	6.70	145 034
120	LR	Resistance	4.06	7.85	145 034
120	RVG	Support	3.84	8.27	145 034
120	RVG	Resistance	3.41	6.81	145 034
N/A	TDST	Support	4.21	7.03	144 314
N/A	TDST	Resistance	4.47	8.00	144 479

Table 11: Full IC on level distance across all windows and horizons. $|t| > 2$ in bold.

W	Method	Level	N	IC	Std	t
20	LR	Support	5	0.003	0.159	0.39
20	LR	Support	10	0.018	0.170	1.69
20	LR	Support	20	0.017	0.173	1.09
20	LR	Resistance	5	0.008	0.166	1.03
20	LR	Resistance	10	0.004	0.169	0.37
20	LR	Resistance	20	−0.007	0.149	−0.52
20	RVG	Support	5	0.004	0.185	0.51
20	RVG	Support	10	0.009	0.184	0.78
20	RVG	Support	20	0.019	0.175	1.18
20	RVG	Resistance	5	0.016	0.188	1.93
20	RVG	Resistance	10	0.019	0.193	1.56
20	RVG	Resistance	20	0.027	0.181	1.63
60	LR	Support	5	0.016	0.178	1.99
60	LR	Support	10	0.022	0.186	1.83
60	LR	Support	20	0.034	0.174	**2.14**
60	LR	Resistance	5	0.008	0.175	1.00
60	LR	Resistance	10	0.011	0.179	0.94
60	LR	Resistance	20	0.014	0.177	0.87
60	RVG	Support	5	0.007	0.191	0.85
60	RVG	Support	10	0.010	0.185	0.87
60	RVG	Support	20	0.019	0.182	1.13
60	RVG	Resistance	5	0.016	0.186	1.92
60	RVG	Resistance	10	0.020	0.181	1.72
60	RVG	Resistance	20	0.021	0.186	1.24
120	LR	Support	5	0.017	0.173	**2.17**
120	LR	Support	10	0.020	0.170	1.87
120	LR	Support	20	0.028	0.159	1.94
120	LR	Resistance	5	0.010	0.180	1.22
120	LR	Resistance	10	0.006	0.173	0.53
120	LR	Resistance	20	0.007	0.171	0.44
120	RVG	Support	5	0.008	0.199	0.91
120	RVG	Support	10	0.012	0.190	1.01
120	RVG	Support	20	0.012	0.194	0.71
120	RVG	Resistance	5	0.011	0.193	1.30
120	RVG	Resistance	10	0.014	0.192	1.12
120	RVG	Resistance	20	0.006	0.191	0.36
N/A	TDST	Support	5	0.006	0.197	0.64
N/A	TDST	Support	10	0.007	0.194	0.59
N/A	TDST	Support	20	0.009	0.194	0.51
N/A	TDST	Resistance	5	0.005	0.194	0.53
N/A	TDST	Resistance	10	0.003	0.190	0.27
N/A	TDST	Resistance	20	0.006	0.189	0.37